SCIENTIFIC COMMITTEE
TWENTIETH REGULAR SESSION

Manila, Philippines
14 – 21 August 2024

Spatial Structure and Regional Connectivity of South Pacific Albacore Tuna in the WCPO and EPO

WCPFC-SC20-2024/SA-IP-04

1 August 2024

Jed Macdonald[1], Giulia Anderson[1], Kyne Krusic-Golub[2], François Prioul[3], Charles Cuewapuru[3], Malo Hosken[1], Vanille Barthelemy[1], Taiana Raoulx[4], Peter Grewe[5], Simon Nicol[1] and Afaiture Panapa[4]

[1] Oceanic Fisheries Programme (OFP), Pacific Community (SPC), Noumea, New Caledonia
[2] Fish Ageing Services, 28 Swanston St, Queenscliff 3225, VIC, Australia
[3] Adecal Technopole/Service du parc naturel de la mer de Corail et de la pêche, Noumea, New Caledonia
[4] Moana Nui Development/Directorate of Marine Resources, Papeete, French Polynesia
[5] The Commonwealth Scientific and Industrial Research Organisation, Australia

Executive Summary

Responding to a recommendation in the 2021 south Pacific albacore assessment presented to SC17, a two-phase study was initiated to improve knowledge on the population structure of the stock across the western and central Pacific Ocean (WCPO) and eastern Pacific Ocean (EPO).

The study takes a holistic approach, using genetic markers coupled with analyses of otolith shape and otolith microchemistry to explore evidence for population differentiation. The specific aims are to i) help inform decisions on the spatial structure for the 2024 assessment (Teears et al. 2024), along with other supporting analyses (Potts et al. 2024), and ii) help guide sampling strategies and analytical pipelines for the current south Pacific albacore close-kin mark-recapture (CKMR) project (WCPFC Project 100c – SPC-OFP and CSIRO 2024). This Information Paper presents results from Phase 1 of the study, involving a broad-scale comparison between the western WCPO (New Caledonia) and the western EPO (French Polynesia).

Analyses of otolith shape and genetic data from sexually mature individuals captured within the New Caledonian EEZ (n = 55) and the French Polynesian EEZ (n = 55) during November 2022 both support the existence of population differentiation between the two sampling locations. Furthermore, genetic data from an additional 38 individuals captured from New Caledonian waters in June 2022 indicate seasonal stability in the New Caledonian population genomic signature over at least a five-month period from June through November (2022). Thus, seasonal variation cannot explain the genetic differentiation observed between fish collected from New Caledonia and French Polynesia.

These results align with movement rate estimates from SEAPODYM used in the 2024 assessment, and together with other lines of evidence, lend support to the 2-region spatial structure adopted this year. That said, questions remain around the precise location of the longitudinal division in the south Pacific albacore stock; specifically, if this lies within the WCFPC-CA 'overlap' region, now part of sub-regions 1D and 1F, or further west or east? And does this division persist latitudinally?

To address these questions, we recommend follow-up work be undertaken on south Pacific albacore population structure. This work could include completion of Phase 1 analyses and refinement of a Phase 2 design that involves finer-scale sampling across the WCPO and further east into the EPO.

We invite SC20 to:

- Note the Phase 1 results presented in this paper.
- Support the 2024 PAW recommendation for follow-up studies of south Pacific albacore population structure, including completion of the otolith microchemistry component of Phase 1 and refinement of a Phase 2 design, that:
    - i) incorporates finer-scale, structured sampling across the WCPO and further east in the EPO;
        - We note that PAW 2024 highlighted the opportunity for EPO sampling by members that operate vessels in that jurisdiction.
        - We invite SC20 to encourage those members to participate in the necessary sample collection, as well as request SPC-OFP to liaise with the IATTC to enable opportunities for collaborative sample collection.
    - ii) combines empirical and modelled data from a variety of sources where available; and
    - iii) explores intrinsic and environmental mechanisms that might give rise to the observed population structure.

- Recognise the value of multiple lines of evidence, as presented here, to:
    i) help inform decisions on spatial structure in tuna stock assessments (sensu Hamer al. 2023); and
    ii) help inform CKMR sampling designs and analytical pipelines for WCPFC Project 100c.

Background

The representation of spatial structure in stock assessment models can have a strong influence on model outputs and subsequent management advice (Hilborn et al. 2003; Cadrin 2020, 2023). Theory, empirical examples and simulation testing indicate that correctly specifying spatial processes can improve model accuracy (Porch et al. 1998; Punt 2019), help align a model's regional boundaries with biology (Cadrin et al. 2014), improve forecasts on how stocks might respond to various management and environmental change scenarios (e.g. Bell et al. 2018) and reduce socio-economic risks associated with overharvesting or eroded spatial population structure (Ciannelli et al. 2013).

Ideally, all available data on the biological and fishery-related factors relevant to a particular species or stock are gathered and contribute to decisions on the preferred spatial structure for a given assessment (see Moore et al. 2020a, b; Hamer et al. 2023). These data can come from a variety of sources informative at different scales. For example, genetic and genomic data can offer inference on population structure at evolutionary timescales (e.g. Grewe et al. 2015; Pecararo et al. 2018; Bravington et al. 2016, 2021). Tag-recapture data (Williams et al. 2018), otoliths (Macdonald et al. 2013; Duncan et al. 2018; Artetxe-Arrate et al. 2021), muscle stable isotopes (Lorrain et al. 2020), parasites (Moore et al., 2019), meristics, fatty acids and morphometrics (e.g. methods based on length frequency analysis) (Lennert-Cody et al. 2010; Xu et al. 2023; Potts et al. 2024) act at the scale of a fish's lifetime and can contribute to continued advancements in population dynamics and simulation-based models (e.g. SEAPODYM – Senina et al. 2020; Ikamoana – Scutt Phillips et al. 2018). Fishery catch data can provide an intra- and inter-generational perspective (Glaser et al. 2011, 2014; Hamer et al. 2023). Combining inference from multiple data types is seen as good practice to uncover population structure in marine fishes (e.g. Brophy et al. 2020; Taillebois et al. 2021) and this would seem a prudent path towards improving estimates of movement and mixing rates for tropical tunas (Moore et al. 2020b). This information could then be used to guide the selection of candidate spatial structures for the assessment model (Hamer et al. 2023).

In the case of south Pacific albacore (*Thunnus alalunga*), while the limited tagging data available do highlight individuals' capacity to undertake long-range latitudinal and longitudinal movements across the south Pacific (Williams et al. 2015, Figure 2 in Castillo-Jordán et al. 2021), analyses of genetic markers (e.g. Takagi et al. 2001; Montes et al. 2012; Anderson et al 2019, but see Laconcha et al. 2015), otolith microchemistry (Macdonald et al. 2013), growth variability (Williams et al. 2012; Farley et al. 2021) and gonad development (Farley et al. 2013) are indicative of population differentiation between the western and easternmost regions of the WCPFC Convention Area (WCPFC-CA) and between the western and central Pacific Ocean (WCPO) and eastern Pacific Ocean (EPO). These results are supported by the latest SEAPODYM solutions for south Pacific albacore that estimate limited exchange of individuals between the WCPO and the EPO (see Senina et al. 2020; SHOU, ANCORS and SPC 2024; Teears et al. 2024). That said, most empirical studies to date have been constrained by a lack of spatial and temporal resolution and/or structured sampling. And, as highlighted in the review by Moore et al. (2020a), substantial uncertainty remains around the scale of longitudinal movements of south Pacific albacore within the WCPO, and the degree of connectivity between WCPO and EPO populations.

This uncertainty around longitudinal movement dynamics led to recommendations from the 2018 pre-assessment workshop (PAW) to investigate a new spatial structure for the 2018 south Pacific albacore stock assessment to simplify the previous model while retaining biological realism (Pilling and Brouwer 2018). Consequently, the 8-region structure spanning the area of the WCPFC-CA south of the equator used in the 2015 assessment (Harley et al. 2015) was simplified to a 5-region structure in 2018 (see Tremblay-Boyer et al. 2018a, b). The 2021 stock assessment presented to SC17 (Castillo-Jordán et al.

2021) made a further simplification to a 3-region structure with no longitudinal breaks within the WCPFC-CA and represented the first attempt at a fully spatially structured assessment for south Pacific albacore spanning both the WCPO and EPO. It noted:

"The most influential uncertainty of those considered in this assessment was the assumption related to movement of fish among the model regions. Further research on albacore movement and population mixing across the entire south Pacific should be a priority. Given the difficulty of tagging albacore, genetic and otolith-based approaches are recommended."

It also noted:

"… the development of the Close Kin Mark Recapture (CKMR) methods that can provide information on population scale and stock structure, along with other fishery-independent information on uncertain biological processes, and we strongly recommend that this approach is considered for south Pacific albacore …"

In response to these recommendations, a two-phase study was initiated to better define the population structure of south Pacific albacore across the WCPO and EPO. The study takes a multidisciplinary approach using population genetics coupled with analyses of otolith morphology and otolith microchemistry, building on previous work that used genetic or otolith-based techniques in isolation (e.g. Williams et al. 2012; Macdonald et al. 2013; Anderson et al. 2019). The specific aims are to i) help inform decisions on the spatial structure for the 2024 Pacific-wide south Pacific albacore assessment (Teears et al. 2024), along with other supporting analyses (Potts et al. 2024), and ii) help guide sampling strategies and analytical pipelines for the south Pacific albacore CKMR project (WCPFC Project 100c - Bravington et al. 2021; SPC-OFP and CSIRO 2024).

This Information Paper briefly outlines the study design and presents results from the first phase of the work.

Study design

The study comprises two phases designed to provide inference at different spatial scales:

Phase 1. Broad-scale comparison

Aims to explore evidence for broad-scale population structure in south Pacific albacore within the WCPFC-CA, specifically between the western WCPO (New Caledonia) and the western EPO (French Polynesia).

Phase 2. Finer-scale comparison

The Phase 2 design is partially contingent upon Phase 1 results. It involves finer-scale sampling across a larger geographic area that covers the core region of south Pacific albacore catch in the WCPO and EPO. The results derived from Phase 2 will help pinpoint where any east-west division lies geographically, as well as adding information to our understanding of latitudinal movement dynamics of potential value for CKMR sampling designs.

Sample collection and analysis for the genetics and otolith shape components of Phase 1 are now complete, and we focus on these aspects in the remainder of the paper.

Methods

Sample collection

During November 2022, SPC staff, working in collaboration with fisheries agencies, fishing companies, and the observer and port sampling programmes in French Polynesia (FP) and New Caledonia (NC) collected muscle tissue samples (for high-throughput genomic analyses) and sagittal otoliths (for ageing and morphological and chemical measurements) from 110 sexually mature albacore tuna (fork length range: 80 to 105 cm) captured in each of the FP (n = 55) and NC (n=55) EEZs, within a one-month time window (Figure 1). This sampling protocol was designed to minimise the potential for i) ontogenetic variation in otolith morphology and/or chemical composition to confound any spatial variation that may be present, and ii) confounding temporal variation in genetic and otolith markers with any spatial variation that may be present. An additional 38 muscle tissue samples were collected in New Caledonian waters in June 2022 (Figure 1). We included these in our genetic sequencing efforts to provide an out-group during analyses and to assess seasonal effects on the genetics results.

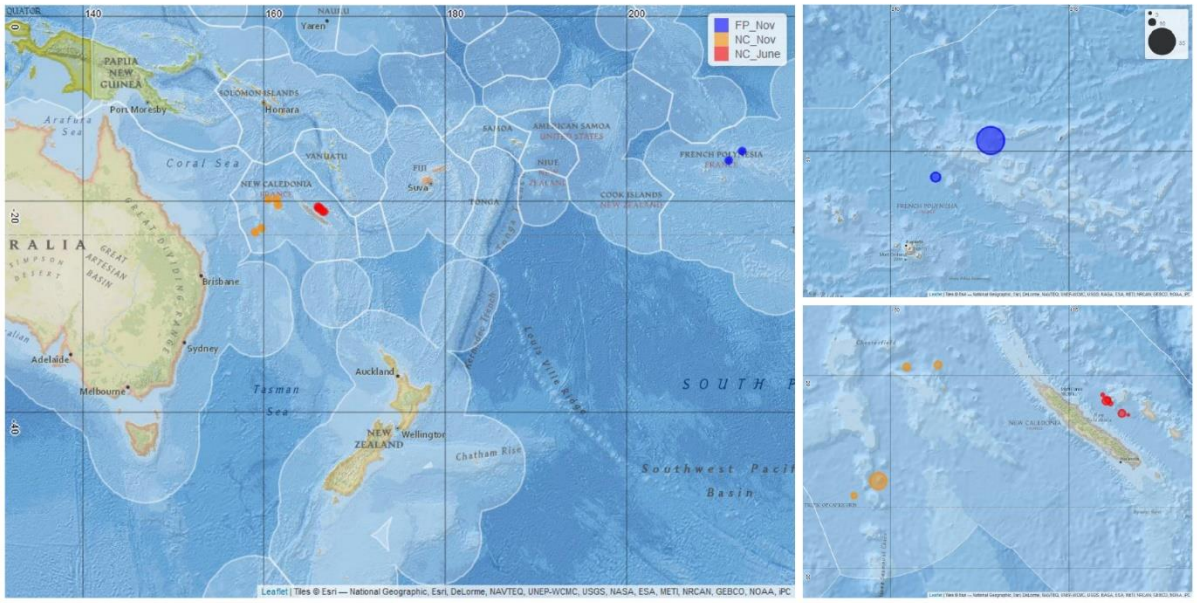

Figure 1. Capture locations for south Pacific albacore in French Polynesian (FP) and New Caledonian (NC) EEZs during June and November 2022. Enlargements of the sampling areas in FP (top right) and NC (bottom right) waters are shown, with circle size in these maps scaled to reflect the sample size per capture location (see black circles at top right for reference).

Muscle tissue samples from fish captured in New Caledonian waters were collected at sea by fisheries observers aboard longline vessels. Fish were sampled on the dorsal musculature just anterior and ventral to the first dorsal spine immediately following capture, using a 3 mm diameter, single-use, medical grade biopsy punch tool (Robbins Instruments). This produced a ~3 × 5 mm tissue sample per fish. Tissue samples were expelled into a sterile 2-ml vial of RNA*later* and stored at −4°C or colder. Each sampled fish's head was then removed and tagged with a cable tie containing a unique ID number before being stored at -20°C or colder for the remainder of the trip. This allowed the tracking of individual fish from vessel to port in Noumea, where the otoliths were extracted, cleaned of adhering tissue and stored dry in labelled vials. In French Polynesia, all fish were sampled in port in Papeete, Tahiti, immediately following unloading from longline vessels. Muscle tissue collection and storage followed the same procedures as for New Caledonia. Otoliths were removed using the drilling method

(https://youtu.be/jbyp_V6C1C0?si=Khfn9Hjs5wjb0tq4) and were cleaned and stored as described above.

Otolith shape analysis

Otolith shape analysis is a well-established approach to uncovering patterns of connectivity and structure in fish populations and has been applied successfully on albacore in the northeast Atlantic (Duncan et al. 2018). We refer readers to Campana and Casselman (1993) and Vignon (2015) for reviews of the mechanisms but note that otolith morphology can be influenced by genetics Cardinale et al. 2004; Vignon and Morat 2010), the environmental conditions experienced throughout life (Hüssy 2008; Berg et al. 2018) and intrinsic processes like somatic growth and feeding history (Hüssy 2008; Denechaud et al. 2020). Several methods have evolved to describe otolith shape. Outline analysis quantifies the boundary shape of the otolith which can be viewed as the lifetime manifestation of the processes mentioned above. We used outline analysis here, requiring only a high-resolution image of each otolith in order to make statistical comparisons of the outlines.

We selected one undamaged otolith per fish (either left or right), photographed the whole otolith under reflected light, sulcus facing down, and measured its mass to the nearest 100 µg. The otolith was then sectioned transversely through the primordium and the fish's age estimated by counting annual growth increments on the resulting thin section. This resulted in age estimates spanning 3 to 11 years across all sampled individuals. Next, we selected fish aged between 4 and 8 years (NC: n = 31; FP: n = 35) as these age classes were the best represented at both sampling locations. Otolith images were first rotated to a standard position, rostrum facing left, and data collected on each otolith's dimensions and outline using the 'shapeR' package (Libungan and Pálsson 2015) in R version 4.3.1 (R Core Team 2023). We measured the maximum length, maximum width, area and perimeter of each otolith, hereafter referred to as 'shape measurements', and detected the outline using the 'detect.outline' function (Claude 2008). To remove size-induced bias, otolith area was normalized to be equal to 1 in all otoliths. We then acquired 64 independent Wavelet coefficients to describe the otolith's outline by conducting a discrete Wavelet transform on equally spaced radii using the 'wavethresh' package (Nason 2022). All shape measurements and Wavelet coefficients were standardised by otolith mass to remove the allometric growth effect on otolith shape. Those showing a significant interaction (at $\alpha = 0.05$) between age class and otolith mass or between sampling location and otolith mass based on analysis of covariance (ANCOVA) were omitted automatically. This step left either three or four shape measurements and 57 Wavelet coefficients for analysis.

To visualise otolith shape variation among age classes and between the two sampling locations (i.e. NC and FP) we used boxplots of shape measurements, reconstructions of mean otolith outlines derived from Wavelet coefficients and ordination results from principal component analyses (PCAs) run in the 'vegan' package (Oksanen et al. 2022). We then tested for an effect of estimated fish age on otolith shape within each sampling location using constrained ordination (i.e. canonical analysis of principal coordinates – CAPs) in 'vegan' and applying an ANOVA-like permutation test to assess the significance of constraints (in this case, fish age) using 1000 permutations. Next, we tested for an effect of sampling location on otolith shape, again using CAP and applying the same permutation test. Finally, we assessed classification accuracy of individuals to their sampling locations in FP and NC based on otolith shape using discriminant analyses of principal components (DAPC) in the 'adegenet' package (Jombart 2008) and random forest (RF) classifiers built in the 'randomForest' package (Liaw and Wiener 2002). The RF hyperparameters were optimised during preliminary tuning, including the 'ntree' argument which we set to 500 across all models. The PCA, CAP, DAPC and RF analyses were run on three different datasets: 1) shape measurements alone, 2) Wavelet coefficients alone and 3) shape measurements

and Wavelet coefficients combined. The analytical pipeline is summarised in Figure 2 and full R code and data to rerun the analysis is available on request.

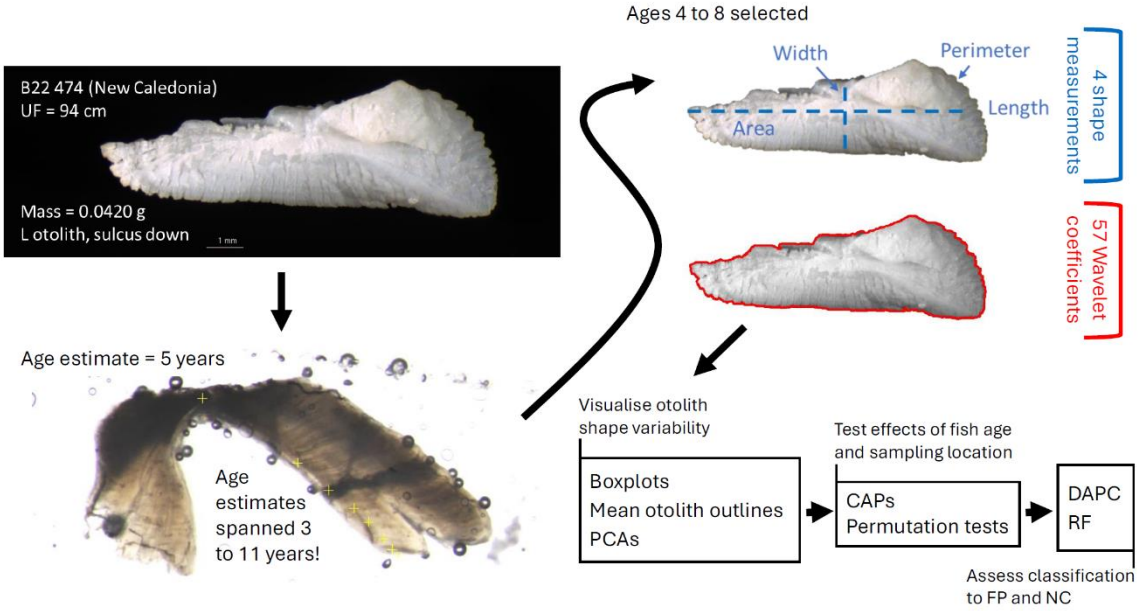

Figure 2. Analytical pipeline for otolith preparation, age estimation and shape analysis. Otolith B22 474 from a 94 cm fork length (UF) south Pacific albacore estimated to be 5 years old is shown for illustration.

Genetic analysis

Genetic samples were sequenced using high-throughput DArTseq protocols by Diversity Arrays Technology, which initially identified over 121,000 loci. The raw dataset was subjected to multiple cycles of quality filters. A fully technical description of the filtering process is available in the Appendix, but in short, we present results from two datasets. The 'primary' dataset includes 6756 datapoints per fish, representing locations from across the genome which were sequenced with very high confidence across all sampled fish. The 'secondary' dataset was further vetted for locations in the genome that carry uncommonly high divergence between FP and NC samples collected in November 2022 (as measured through F_{ST} outlier analyses and disregarding the auxillary sample group during the selection process) to distil patterns of population structure that are otherwise lost in the primary dataset due to the large number of datapoints. The secondary dataset uses 128 datapoints per fish.

The primary dataset was submitted to heterozygosity assessments (which provide population health metrics and are values upon which any other analyses are built) and pairwise comparisons of allele frequencies (which produce single values to quantify degree of difference in genetic signatures between sample groups) using the 'DartRverse' family of packages and StAMPP in R. Various clustering analyses (which employ different assumptions and metrics to reorganise samples into 'logical' groups based on their genetic information) were employed including STRUCTURE, Admixture, and Discriminant Analyses of Principal Components (DAPC, same as is applied to otoliths). Due to its highly selective nature, the secondary dataset was not submitted to heterozygosity assessments, but was submitted to all pairwise and clustering analyses. An additional clustering analysis, StockR, was only applied to the secondary dataset because its algorithm is well designed for marine species but does not include an explicit recommendation for the best number of clusters to report. Again, a full technical description of the genetic analyses can be found in the Appendix.

Results

Otolith shape analysis

Effects of fish age on otolith shape

We detected only subtle differences in otolith shape among age classes for 4- to 8-year-old south Pacific albacore within each sampling location based on standardised shape measurements (Figure A1B) and reconstructions of mean otolith outline per age class from Wavelet coefficients (Figures A1A). These differences were not statistically significant (at $\alpha = 0.05$) for all three datasets (Table 1). The PCA plots in Figure 3C further illustrate the lack of pattern among age classes within sampling locations for all three datasets. Based on these findings. we deemed it appropriate to pool samples from fish aged 4 to 8 within each location for the spatial comparisons between FP and NC.

Table 1. Results from analysis of variance (ANOVA)-like permutation tests of otolith shape variation among age classes within sampling locations, and between sampling locations (when all age classes were pooled within locations). We used 1000 permutations to assess the significance of constraints. d.f. = degrees of freedom; Variance = variance among levels of the constraint; values for Sum of Squares denoted with an *; *F* = pseudo *F*-value (Oksanen et al. 2022).

Tested constraint	Sampling location	Dataset	d.f.	Variance / Sum of squares*	*F*	*p*
Age Residual	FP	Shape measurements	4 30	0.491 2.066	1.782	0.118
	FP	Wavelet coefficients	4 30	5.556* 30.141	1.383	0.102
	FP	Combined	4 30	0.654 2.953	1.662	0.112
	NC	Shape measurements	3 27	0.338 7.081	0.430	0.760
	NC	Wavelet coefficients	3 27	3.479* 31.795	0.702	0.803
	NC	Combined	3 27	0.421 0.1408	0.4655	0.780
Sampling location Residual	-	Shape measurements	1 64	0.096 2.946	2.084	0.126
	-	Wavelet coefficients	1 64	1.833* 65.220	1.798	0.080
	-	Combined	1 64	0.124 3.950	2.011	0.093

Effects of sampling location on otolith shape

With reference to Figure 3, we see that FP and NC otoliths differed in standardised length and perimeter, with NC samples consistently smaller in these dimensions (Figure 3B). The reconstructions of mean otolith outline revealed most of the variation among sampling locations to be between 135° and 170° along the dorsal otolith edge near the rostrum (Figure 3B). The ordination plots (Figure 3C) showed no strong patterns between the two sampling locations along the first two principal components for all three datasets, though the permutation test results (Table 1) do suggest a degree of statistical differentiation between sampling locations driven primarily by variation in Wavelet coefficients. This differentiation is also evident in the density distributions plotted along the first discriminant function of the DAPC run on each dataset (Figure 4).

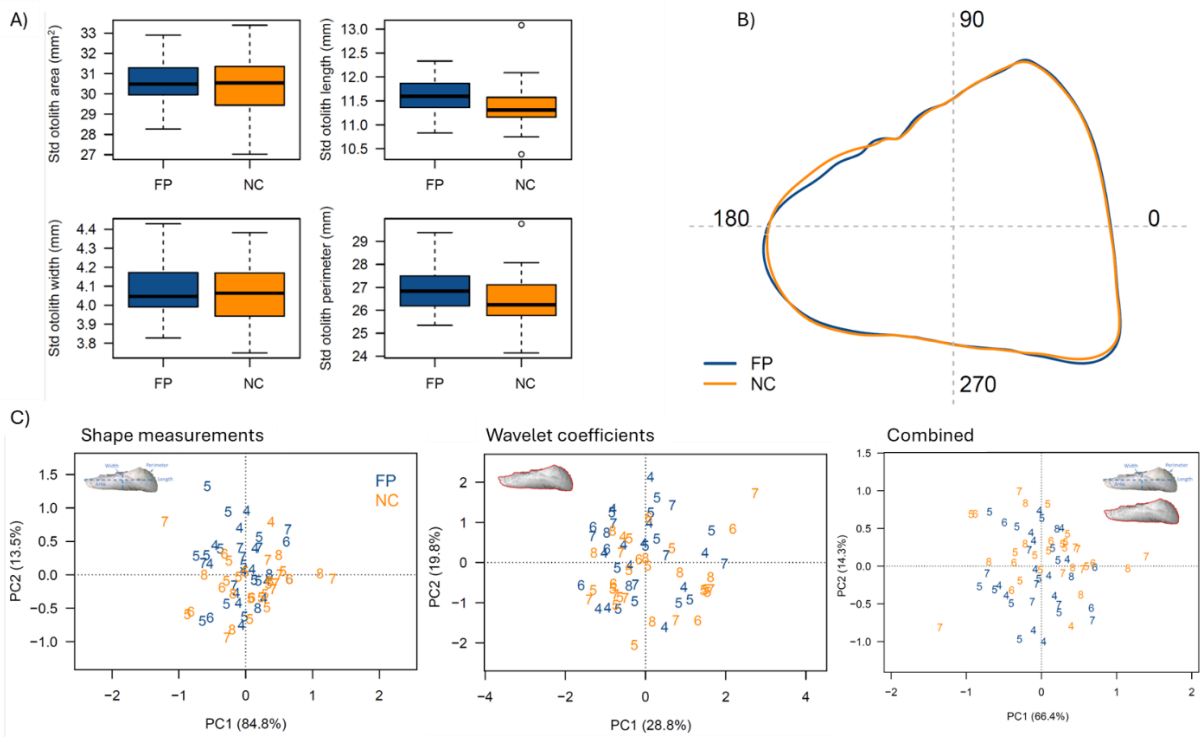

Figure 3. Visualisation of otolith shape variation between sampling locations in FP and NC. A) Box plots summarising the distribution of standardised shape measurements per sampling location. Thick black horizontal lines are the median values for each box and the lower (Q1) and upper (Q3) quartiles (box limits) are shown. Upper whiskers represent the smaller of the maximum value of the variable and Q3 + 1.5 × interquartile range, and lower whiskers the larger of the minimum value of the variable and Q1 - 1.5 × interquartile range. B) Mean reconstructed otolith outline for each sampling location. Numbers refer to angles in degrees. C) Ordination plots describe variation along the first two principal components (PCs) for the three different datasets used. The variance explained by each PC is shown on the axes. The numbers in the ordination plots reflect the age estimate from counts of annual growth increments on a thin section of the same otolith. In all plots, samples from FP are shown in blue, NC in orange.

Regarding classification accuracy, the DAPC on the shape measurements alone showed that, overall, 68.2% of individuals were reassigned correctly to their sampling location. A leave-one-out cross validation (LOO-CV) procedure produced higher misclassification rates (Table 2). The DAPC run on the Wavelet coefficients alone returned a classification success rate of ~60%. Again, LOO-CV classification success was lower. When we combined the shape measurements and Wavelet coefficients, LOO-CV classification success improved to 63.6%. 'Out-of-bag' estimates of classification success on 36.8% of the data held out from training the RF classifiers were similar to the DAPC estimates (Table 2). For both DAPC and RF models, samples from FP were always more accurately classified than NC samples.

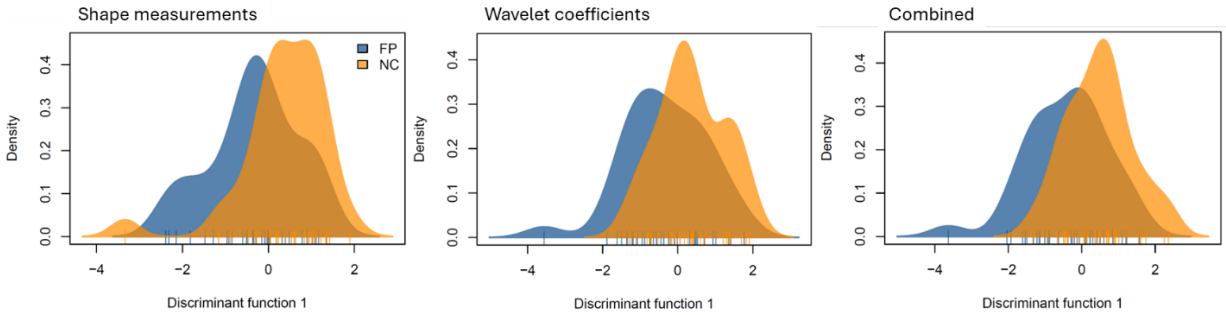

Figure 4. Density distributions for each sampling location along the first discriminant function derived from DAPCs run on each of the three datasets. Samples from FP are shown as blue tick marks on the rug plot, samples from NC are shown as orange tick marks.

Table 2. Percentage of individuals correctly re-assigned to their sampling location based on DAPC and RF classifiers for each of the three datasets. 'all data' = classification based on all data from FP and NC; 'LOO-CV' = leave-one-out cross validation; 'OOB' = out-of-bag; 'FP' = classification based on FP data alone; 'NC' = classification based on NC data alone.

Classification model	Shape measurements	Wavelet coefficients	Combined
DAPC - all data	68	61	67
DAPC - all data LOO-CV	59	55	64
DAPC - FP	71	66	71
DAPC - NC	65	55	61
RF - all data OOB	65	52	62
RF - FP OOB	69	57	71
RF - NC OOB	61	45	52

Genetic analysis

As a reminder, genetic analyses also include an out-group collected in New Caledonia in June 2022 (Figure 1). We therefore label our groups with the added month specificity. Namely, the primary groups are FP_Nov and NC_Nov, and we refer to the additional group as NC_June. We refer to the quality-filtered, genome-wide dataset as 'primary' and the smaller dataset that was filtered for quality and informativeness as 'secondary'.

Heterozygosity-based assessments like observed (H_o), adjusted expected heterozygosity (H_e) and inbreeding coefficient (F_{IS}) provide some general information about the robustness of genetic diversity per sample group and allow for comparisons between groups (lower diversity metrics can imply a smaller or less robust underlying population). Results of these analyses using the primary dataset are provided in Table 3. Pairwise assessment of a related heterozygosity metric, F_{ST}, which quantifies differences in genetic signature on a scale of 0-1, is provided in Table 4. Of key interest, FP_Nov and NC_Nov produced a pairwise F_{ST} value of 0.006 (adjusted p-value = 0) while the two NC samples are not statistically different.

Table 3. Heterozygosity-based metrics with standard deviation in parentheses produced using the primary dataset.

	H_o	H_e	F_{IS}
FP_Nov	0.1321 (0.1196)	0.1505 (0.1343)	0.0986 (0.2238)
NC_June	0.1343 (0.1210)	0.1511 (0.1334)	0.0903 (0.2308)
NC_Nov	0.1302 (0.1176)	0.1491 (0.1330)	0.1028 (0.2267)

Table 4. Pairwise F_{ST} from the primary dataset with metrics provided below the diagonal. Associated p-values adjusted for multiple comparisons using the Benjamini and Yekutieli (2001) method are reported above the diagonal.

	F_{ST}		
	FP_Nov	NC_June	NC_Nov
FP_Nov	---	0	0
NC_June	0.0052	---	0.6892
NC_Nov	0.0058	0.00011	---

We also applied three clustering algorithms to the primary dataset and all concurred on a recommended *k* of 1, suggesting a single population underlies all three sample groups (Figure 5). However, a DAPC identified enough variation to separate the two primary sample groups using 40 principal components (Figure 6).

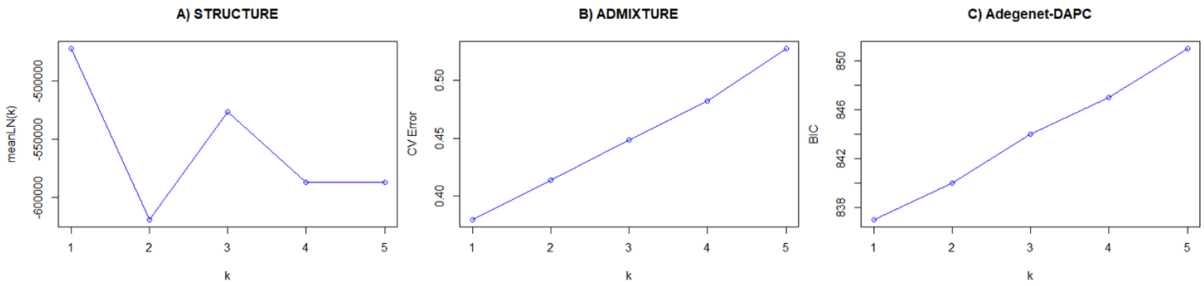

Figure 5. Results from submitting the primary dataset to three clustering programs with different metrics for selecting the most appropriate number of underlying genetic clusters. A) STRUCTURE, where the recommended k is indicated by a plateau in average posterior probability (LnP(K)) and non-convergence suggests *k*=1, B) ADMIXTURE, in which a minimum CV error defines the recommended *k*, and C) DAPC clustering, which recommends the appropriate *k* based on the lowest Bayesian Information Criterion (BIC) value.

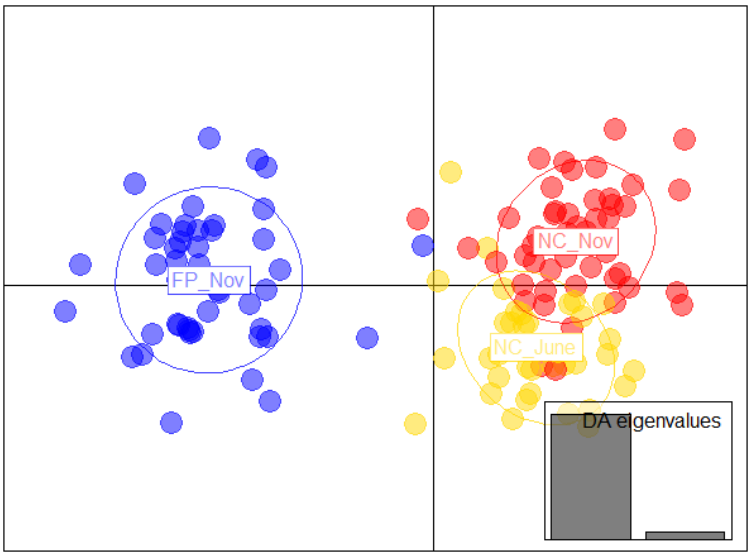

Figure 6. DAPC on the primary genetic dataset using 40 PCs (number of PCs informed by cross-validation) and 2 degrees of freedom

Meanwhile, using the specially selected secondary dataset, heterozygosity assessments were not conducted but we still tested for pairwise F_{ST} (Table 5). Clustering algorithms consistently recommended a *k* of 2 (Figure 7), with subsequent assignment probability analyses (which reassign individuals to the theoretical genetic clusters developed by clustering algorithms) identifying at most three instances of specimens that did not agree with their original geographic groupings (Figure 8, panels A-C). Similarly, a DAPC, which visually groups individuals based on genetic similarity but is not driven by k-clustering, maintains a clear overlap between the two NC sample groups and distinction from the FP samples (Figure 8, panel D). We also note the addition of a result from StockR in Figure 8 (panel C), which produces comparable results using underlying assumptions that are particularly well suited for marine species.

Table 5. Pairwise F_{ST} using the secondary dataset. Values are presented as in Table 4.

	F_{ST}		
	FP_Nov	NC_June	NC_Nov
FP_Nov	---	0	0
NC_June	0.1426	---	0.0029
NC_Nov	0.1581	0.0086	---

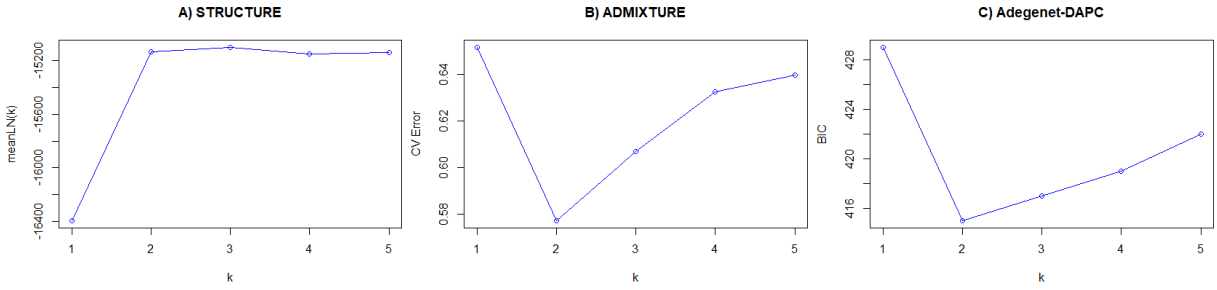

Figure 7. Results from submitting the secondary dataset to three clustering programs. A) STRUCTURE, B) ADMIXTURE, and C) Adegenet-DAPC. Same metrics described as in Figure 5.

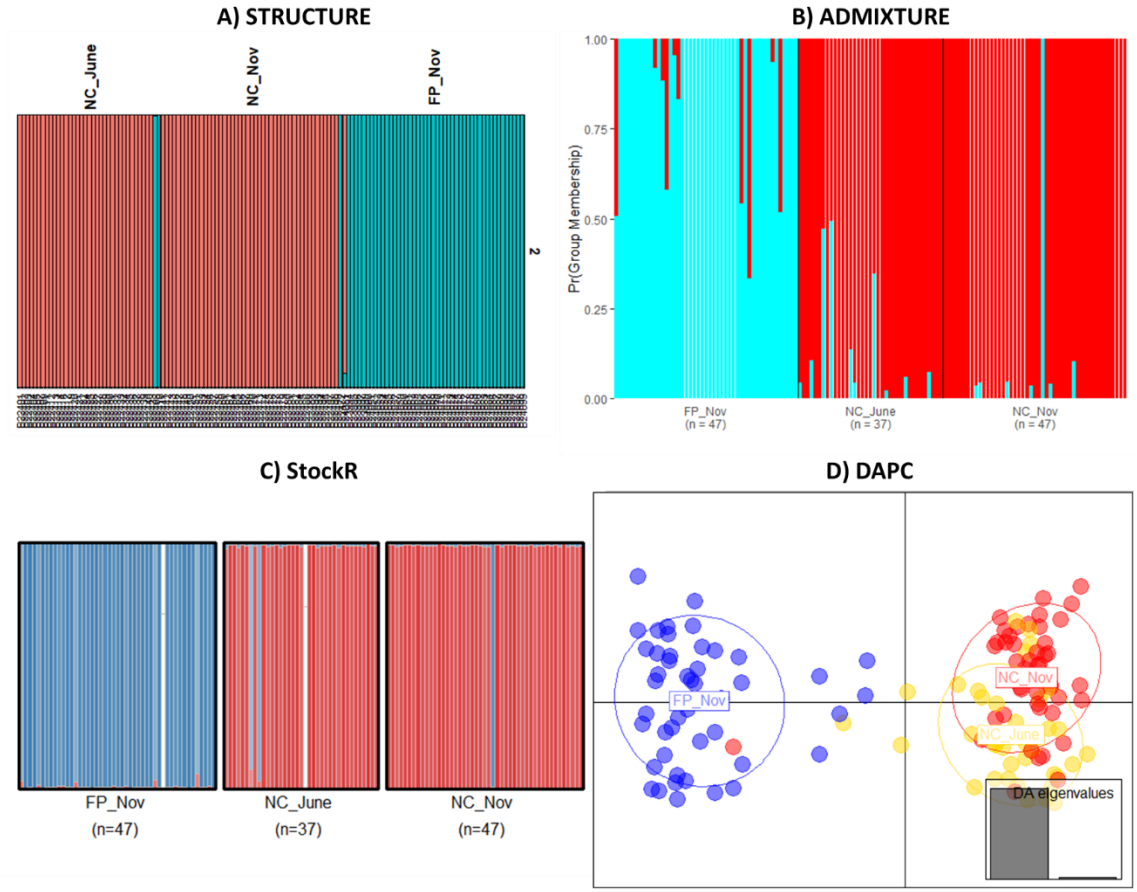

Figure 8. Individual allocations using the secondary dataset by clustering programs given *k* = 2. A) STRUCTURE, where bars represent an individual's probability of assignment to each color-coded cluster, with mixed colored individuals suggesting admixture. B) ADMIXTURE, with same representation as STRUCTURE but constructed using different algorithms. C) StockR, multi-colored bars now represent probability of assignment (not mixed heritage) and colour intensity reflects confidence of assignment. D) DAPC using 10 principal components and 2 discriminant functions.

Discussion

The results from Phase 1 of the study provide strong evidence for the existence of broad-scale population structure in south Pacific albacore between the western WCPO (New Caledonia) and the western EPO (French Polynesia). Moreover, the stability detected in the New Caledonian population genomic signature between June and November 2022 highlights that seasonal variation cannot explain the spatial differentiation we observed between fish collected from New Caledonia and French Polynesia. While acknowledging the small sample sizes available for our comparisons, the agreement observed between the otolith shape and genetic results is notable, particularly as these data types provide inference at different temporal scales and are underpinned by different mechanisms. Taken together, our findings support previous interpretations of the extent of longitudinal structure present within the south Pacific albacore stock based upon analyses of genetic and otolith microchemistry data in isolation (e.g. Montes et al. 2012; Anderson et al. 2019; Macdonald et al. 2013), growth variation and reproductive development (Williams et al. 2012; Farley et al. 2013, 2021) and modelled movement estimates (Senina et al. 2020; SHOU, ANCORS and SPC 2024; Teears et al. 2024).

The Phase 1 sampling protocol – targeting mature south Pacific albacore of 80 cm fork length or larger within the same one-month window in both sampling locations – aimed to minimise potential bias related to ontogenetic and/or temporal variation in otolith and genetic markers that could confound our interpretation of geographic variation in these markers between FP and NC. Despite achieving these sampling objectives, the large range of ages (i.e. 3 to 11 years) estimated for our sampled fish necessitated a test for age effects within each sampling location as a first step in the otolith shape analysis. We detected only subtle differences in mean otolith outlines among age classes for 4- to 8-year-old individuals when shape descriptors were standardised by otolith mass[6], allowing data to be pooled across age classes within sampling locations. Importantly, subsequent spatial comparisons using permutation tests, DAPC and RF classifiers on the range of shape descriptors analysed were all in agreement, indicating a degree of differentiation between FP and NC samples.

Otolith outlines can be viewed as life-time representations of both the intrinsic (e.g. genetics, somatic growth rate, fish size, feeding history) and environmental factors (e.g. temperature, depth, prey availability) experienced by individual fish (Cardinale et al. 2004; Hüssy 2008; Vignon and Morat 2010; Denechaud et al. 2020). While distinguishing the relative contribution of these factors remains challenging (Vignon 2015), it is increasingly recognised that allometry is a key determinant, and that the experienced environment can act indirectly – via dictating patterns of growth increment formation throughout life which in turn strongly influence otolith morphology (Campana and Casselman 1993; Cardinale et al. 2004; Vignon 2015; Denechaud et al. 2020).

With these points in mind, we propose three scenarios that could potentially give rise to the variation we observed in shape descriptors between FP and NC and that could be further explored in a Phase 2 of the study. The first has an environmental basis – juveniles from a single spawning stock following divergent migration pathways in the WCPO and EPO, traversing environment gradients different enough to induce some morphological differences in adult otolith outline. Yet given the genetics results presented herein and in previous work (Takagi et al. 2001; Montes et al. 2012; Anderson et al. 2019), the single spawning stock hypothesis for south Pacific albacore seems highly unlikely (is not genetically possible). A second and more likely explanation involves two (or more) geographically distinct spawning groups with very limited mixing between reproductive spawning aggregations that are exposed to moderately different environmental forces across the lifetimes of group members, as enforced by local and/or regional oceanography. Third, assuming the existence of two (or more) spawning groups, the spatial differences we see could have a genetic basis (Cardinale et al. 2004; Berg et al. 2018) or arise through genetic differences mediated by differences in environmental exposure (Vignon and Morat 2010).

Seeking evidence for each of these scenarios requires additional data. In particular, further work is required to understand oceanographic processes in the south Pacific and north Pacific Tropical Gyres, which bring juveniles to the New Zealand troll fishery. Moreover, there is a need to resolve the ecological and evolutionary connections between juveniles and adults in the EPO and mixing rates between eastern EPO and WCPO populations, noting that samples from juveniles in the EPO have historically been difficult to obtain due to lower fishing activity in that region (SHOU, ANCORS and SPC 2024). Otolith microchemistry data may offer useful insights, generating a time-stamped, individual-

[6] Standardisation by fish length or otolith length is commonly used to account for the allometric growth effect on otolith shape (see Cardinale et al. 2004; Libungan et al. 2015). Our decision to use otolith mass instead was driven by i) the tight relationship observed between fork length and otolith mass for our samples and ii) higher confidence in the accuracy of the otolith weight measurements compared with some uncertainties around some fork length measurements recorded in the field. We note that our results were insensitive to using either fish length or otolith mass for standardisation.

level record of environmental and physiological experience. This approach has proved informative in past studies of movement and mixing in south Pacific albacore (Macdonald et al. 2013). Importantly, it complements other empirical and simulation-based approaches (Sakamoto et al. 2019; Brophy et al. 2020; Taillebois et al. 2022), letting us track connections among individuals and populations at specific life history phases (e.g. hatching, spawning). The otolith microchemistry component of Phase 1 is yet to be completed, and we recommend pursuing this, as well as follow-up studies like that outlined in Phase 2, which extends the Phase 1 design through finer-scale sampling across the WCPO and into the eastern EPO. Following these recommendations would have the dual benefit of informing on the mechanisms driving population structure across the region and guiding aspects of the CKMR design work.

The Phase 1 genetic results come to a similar conclusion as the otolith shape results using different biological mechanisms and timescales. Namely, the data supports the presence of biologically important population structure between FP and NC. Although some of our evidence may seem to contradict this conclusion (namely clustering algorithms that support a single underlying population using the primary dataset) it is a matter of terminology—the presence of structure being different from the presence of discrete populations. The 'primary' dataset, which captures genome-wide differentiation between sample groups, still accurately separates samples by location via DAPC and produces statistically significant differences in group genetic signature via pairwise F_{ST}. Furthermore, the comparison of the two NC sample groups in both analyses quantifies the degree of stochastic differentiation one could expect when sampling the same (sub)population twice, which is a magnitude lower than FP-NC comparisons and not statistically significant.

We also present results from the 'secondary' genetic dataset, which is a distillation of F_{ST} outlier datapoints. We emphasise the risk of misrepresenting larger trends when cherry-picking 2% of available datapoints and limit our interpretation to two points. First, the French Polynesian-New Caledonian structure reported by pairwise F_{ST} and DAPC in the primary dataset is further supported by the individual reassignment steps of all clustering algorithms (a step that is uninformative using the primary dataset, given that the recommended number of underlying populations is one). Second, due to the nature of F_{ST} outlier-based selection, there is an increased chance that the parts of the genome involved may experience adaptive pressure, such as from environmental stressors. Identifying environmental drivers of population structure is a very useful step towards describing the larger population dynamics, and the existence of loci showing outlier patterns of allele frequency distribution suggests it would be worthwhile to consider a follow-up study that captures environmental as well as geographic variation.

These results are consistent with the literature. Our primary and secondary datasets are comparable to neutral and potentially adaptive datasets, respectively, in two other papers that have applied Next Generation Sequencing technology to Pacific albacore stocks (Anderson et al 2019, Vaux et al 2021). In both a west-central South Pacific comparison and North-South Pacific comparison, strong patterns of population structure were reported using potentially adaptive datasets, while the signal was much weaker using neutral datasets.

Like the otolith shape dataset, we note that the current genetics datasets are not equipped to propose a complete theory about the state of population structure in the south Pacific or what the exact drivers are. As stated above, we therefore recommend undertaking Phase 2 of the study to more thoroughly explore the correlation of genetic and otolith variation with various environmental forcings. From a genetics standpoint, we would particularly encourage the collection of samples from still further east in the EPO, as a way to capture more divergent environmental conditions that may better clarify drivers of adaptive population structure.

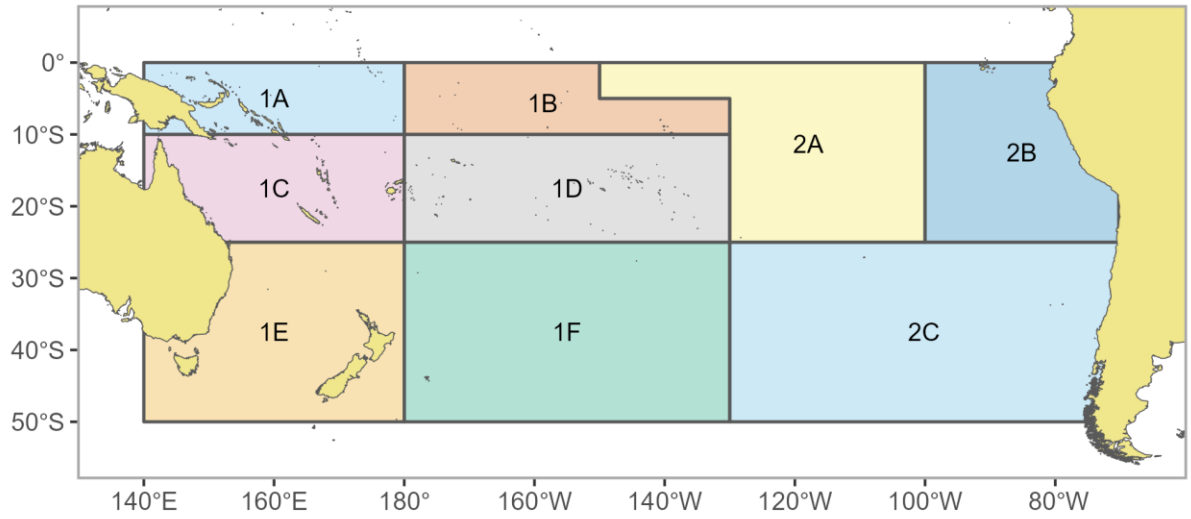

Figure 9. Spatial structure used in the 2024 south Pacific albacore assessment. Numbers 1 and 2 indicate explicit regions in the assessment model. The letters (A, B, etc) indicate sub-regions used for the definition of fisheries (redrawn from Teears et al. 2024).

Do our findings support the 2024 spatial structure?

Some discussion is also warranted on how our results align with the spatial structure chosen for the 2024 south Pacific albacore assessment. The 2024 assessment uses a simplification of the 4-region structure used in the 2021 assessment (Castillo-Jordán et al. 2021) to a 2-region structure with sub-regions defined by fisheries (Figure 9). Region 1 corresponds to the area of the WCPO within the WCPFC-CA from the equator to 50°S, including the 'overlap' region, while region 2 encompasses the same latitudes in the EPO, within the Inter American Tropical Tuna Commission (IATTC) Convention Area, excluding the overlap region (Figure 9).

Movement between regions 1 and 2 is estimated as age and season specific. In the absence of informative tag-recapture data, particularly in relation to longitudinal movement rates, the 2024 PAW proposed the use of the SEAPODYM model to provide information on recruitment distribution and movement rates across life stages (Senina et al. 2020, Hamer 2024 [SC20-2024/SA-IP-01]). This plan was adopted in the 2024 assessment (Teears et al. 2024). In summary, SEAPODYM estimated low movement rates between regions 1 and 2 across all age classes, with negligible influence of season on these estimates. Four additional sensitivities to the movement specification were considered i) zero movement between the WCPO and EPO regions, and ii) lower movement (i.e. movement probabilities half those estimated by SEAPODYM), iii) higher movement (i.e. movement probabilities double those estimated by SEAPODYM) and iv) movement approximating full and instantaneous mixing of the stock. Sensitivities i) and iv) were not considered biologically plausible; however, these were included in the sensitivity runs as extreme lower and upper limits. Overall, the stock assessment results appeared to be robust to the movement assumption and it was deemed unnecessary to consider alternative movement scenarios in the final model ensemble (Teears et al. 2024).

Our empirical findings are in line with the SEAPODYM estimates, noting that the Phase 1 sampling coverage only encompasses the overlap region of the EPO and not further east, whereas SEAPODYM estimates are calculated across the entire assessment domain. Moreover, our findings, in conjunction with other lines of evidence (Williams et al. 2012; Farley et al. 2013, 2021; Takagi et al. 2001; Montes

et al. 2012; Macdonald et al. 2013; Anderson et al. 2019; Potts et al. 2024) largely support the chosen 2-region structure for the 2024 assessment. That said, important questions remain around the precise location of the longitudinal division in the south Pacific stock; specifically, if this lies within the WCFPC-CA overlap region, now part of sub-regions 1D and 1F, or further west or east? And does this division persist latitudinally? A Phase 2 of the study, incorporating finer-scale sampling across a broader region of the WCPO and EPO and integrating other empirical and modelled data where available, would help to answer these questions.

Recommendations

We invite SC20 to:

- Note the Phase 1 results presented in this paper.
- Support the 2024 PAW recommendation for follow-up studies of south Pacific albacore population structure, including completion of the otolith microchemistry component of Phase 1 and refinement of a Phase 2 design, that:
    iv) incorporates finer-scale, structured sampling across the WCPO and further east in the EPO;
        – We note that PAW 2024 highlighted the opportunity for EPO sampling by members that operate vessels in that jurisdiction.
        – We invite SC20 to encourage those members to participate in the necessary sample collection, as well as request SPC-OFP to liaise with the IATTC to enable opportunities for collaborative sample collection.
    v) combines empirical and modelled data from a variety of sources where available; and
    vi) explores intrinsic and environmental mechanisms that might give rise to the observed population structure.
- Recognise the value of multiple lines of evidence, as presented here, to:
    i) help inform decisions on spatial structure in tuna stock assessments (sensu Hamer al. 2023); and
    ii) help inform CKMR sampling designs and analytical pipelines for WCPFC Project 100c.

Acknowledgements

We thank Franck, Suane and the team at ALBACORE SARL, as well as the fishing vessel captains and crews unloading in Papeete port, French Polynesia, for their interest and cooperation with sampling efforts. Thanks also to Sylvain Taataroa (Moana Nui Development) and Thibaut Thellier (Directorate of Marine Resources, French Polynesia) for support with logistics and sampling in Papeete port.

References

Anderson, G., Hampton, J., Smith, N., and Rico, C. 2019. Indications of strong adaptive population genetic structure in albacore tuna (*Thunnus alalunga*) in the southwest and central Pacific Ocean. Ecology and Evolution, 9: 10354–10364.

Artetxe-Arrate, I., Fraile, I., Farley, J., Darnaude, A. M., Clear, N., Rodríguez-Ezpeleta, N., Dettman, D. L., et al. 2021. Otolith chemical fingerprints of skipjack tuna (*Katsuwonus pelamis*) in the Indian Ocean: First insights into stock structure delineation. PLoS ONE, 16(3): e0249327.

Bell, J., Allain, V., Sen Gupta, A., Johnson, J., Hampton, J., Hobday, A., Lehodey, P., et al. 2018. Climate change impacts, vulnerabilities and adaptations: Western and Central Pacific Ocean marine fisheries. In Impacts of climate change on fisheries and aquaculture - Synthesis of current knowledge, adaptation and mitigation options, pp. 305–324. Ed. by M. Barange, T. Bahri, M. Beveridge, K. Cochrane, S. Funge-Smith, and F. Poulain. FAO.

Berg, F., Almeland, O. W., Skadal, J., Slotte, A., Andersson, L., and Folkvord, A. 2018. Genetic factors have a major effect on growth, number of vertebrae and otolith shape in Atlantic herring (*Clupea harengus*). PLoS ONE, 13(1): e0190995.

Bravington, M. V., Skaug, H. J., and Anderson, E. C. 2016. Close-kin mark-recapture. Statistical Science, 31: 259–274.

Bravington, M., Nicol, S., Anderson, G., Farley, J., Hampton, J., Castillo-Jordán, C., and Macdonald, J. 2021. South Pacific Albacore Close-Kin Mark-Recapture: update on design (Project 100b). SC17/SA-IP-14. Seventeenth Regular Session of the Scientific Committee of the Western and Central Pacific Fisheries Commission. Online meeting, 11-19 August 2021. https://meetings.wcpfc.int/node/12572

Brophy, D., Rodríguez-Ezpeleta, N., Fraile, I., and Arrizabalaga, H. 2020. Combining genetic markers with stable isotopes in otoliths reveals complexity in the stock structure of Atlantic bluefin tuna (*Thunnus thynnus*). Scientific Reports, 10:14675.

Cadrin, S. X. 2020. Defining spatial structure for fishery stock assessment. Fisheries Research, 221: 105397.

Cadrin, S. X., Goethel, D. R., Berger, A., and Jardim, E. 2023. Best practices for defining spatial boundaries and spatial structure in stock assessment. Fisheries Research, 262: 106650.

Cadrin, S. X., Kerr, L. A., and Mariani, S. 2014. Interdisciplinary Evaluation of Spatial Population Structure for Definition of Fishery Management Units. In Stock Identification Methods: Applications in Fishery Science: Second Edition, pp. 535–552.

Campana, S. E., and Casselman, J. M. 1993. Stock discrimination using otolith shape analysis. Canadian Journal of Fisheries and Aquatic Sciences, 50: 1062–1066.

Cardinale, M., Doering-Arjes, P., Kastowsky, M., and Mosegaard, H. 2004. Effects of sex, stock, and environment on the shape of known-age Atlantic cod (*Gadus morhua*) otoliths. Canadian Journal of Fisheries and Aquatic Sciences, 61: 158–167.

Castillo-Jordán, C., Hampton, J., Ducharme-Barth, N., Xu, H., Vidal, T., Williams, P., Scott, F., Pilling, G., and Hamer, P. 2021. Stock assessment of South Pacific albacore tuna. SC17/SA-WP-02. Seventeenth Regular Session of the Scientific Committee of the Western and Central Pacific Fisheries Commission. Online meeting, 11-19 August 2021. https://meetings.wcpfc.int/node/12551

Ciannelli, L., Fisher, J. A. D., Skern-Mauritzen, M., Hunsicker, M. E., Hidalgo, M., Frank, K. T., and Bailey, K. M. 2013. Theory, consequences and evidence of eroding population spatial structure in harvested marine fishes: a review. Marine Ecology Progress Series, 480: 227–243.

Claude, J. 2008. Morphometrics with R. Springer, New York, USA, pp. 316.

Denechaud, C., Smoliński, S., Geffen, A. J., and Godiksen, J. A. 2020. Long-Term temporal stability of Northeast Arctic cod (*Gadus morhua*) otolith morphology. ICES Journal of Marine Science, 77: 1043–1054.

Diaz-Arce, N., Gagnaire, P.-A., Richardson, D., Walter, J., Arnaud-Haond, S., Fromentin, J.-M., Brophy, D., et al. 2023. Unidirectional trans-Atlantic gene flow and a mixed spawning area shape the genetic connectivity of Atlantic bluefin tuna. Molecular Ecology, 33(1): e17188.

Duncan, R., Brophy, D., and Arrizabalaga, H. 2018. Otolith shape analysis as a tool for stock separation of albacore tuna feeding in the Northeast Atlantic. Fisheries Research, 200: 68–74.

Farley, J., Krusic-Golub, K., and Eveson, P. 2021. Updating age and growth parameters for South Pacific albacore (Project 106). SC17-SA-IP-10. Seventeenth Regular Session of the Scientific Committee of the Western and Central Pacific Fisheries Commission. Online meeting, 11-19 August 2021. https://meetings.wcpfc.int/node/12568

Farley, J. H., Williams, A. J., Clear, N. P., Davies, C. R., and Nicol, S. J. 2013. Age estimation and validation for South Pacific albacore *Thunnus alalunga*. Journal of Fish Biology, 82: 1523–1544.

Glaser, S. M., Ye, H., Maunder, M., MacCall, A., Fogarty, M., and Sugihara, G. 2011. Detecting and forecasting complex nonlinear dynamics in spatially structured catch-per-unit effort time series for North Pacific albacore (*Thunnus alalunga*). Canadian Journal of Fisheries and Aquatic Sciences, 68: 400–412.

Glaser, S. M., Fogarty, M. J., Liu, H., Altman, I., Hsieh, C. H., Kaufman, L., Maccall, A. D., et al. 2014. Complex dynamics may limit prediction in marine fisheries. Fish and Fisheries, 15: 616–633.

Grewe, P. M., Feutry, P., Hill, P. L., Gunasekera, R. M., Schaefer, K. M., Itano, D. G., Fuller, D. W., et al. 2015. Evidence of discrete yellowfin tuna (*Thunnus albacares*) populations demands rethink of management for this globally important resource. Scientific Reports, 5: 16916.

Hamer, P. 2024. Summary Report from the 2024 SPC Pre-assessment Workshop. SC20/SA-IP-01. Twentieth Regular Session of the Scientific Committee of the Western and Central Pacific Fisheries Commission. Manila, Philippines, 14-21 August 2024. https://meetings.wcpfc.int/node/23085

Hamer, P., Macdonald, J., Potts, J., Vidal, T., Teears, T., and Senina, I. 2023. Review and analyses to inform conceptual models of population structure and spatial stratification of bigeye and yellowfin tuna assessments in the Western and Central Pacific Ocean. SC19/SA-WP-02. Nineteenth Regular Session of the Scientific Committee of the Western and Central Pacific Fisheries Commission. Koror, Palau, 16-24 August 2023. https://meetings.wcpfc.int/node/19350

Hilborn, R., Quinn, T. P., Schindler, D. E., and Rogers, D. E. 2003. Biocomplexity and fisheries sustainability. Proceedings of the National Academy of Sciences, 100: 6564–6568.

Hüssy, K. 2008. Otolith shape in juvenile cod (*Gadus morhua*): Ontogenetic and environmental effects. Journal of Experimental Marine Biology and Ecology, 364: 35–41.

Jombart, T. 2008. adegenet: a R package for the multivariate analysis of genetic markers. Bioinformatics, 24: 1403–1405.

Laconcha, U., Iriondo, M., Arrizabalaga, H., Manzano, C., Markaide, P., Montes, I., Zarraonaindia, I., et al. 2015. New nuclear SNP markers unravel the genetic structure and effective population size of albacore tuna (*Thunnus alalunga*). PLoS ONE, 10(6): e0128247.

Lennert-Cody, C. E., Minami, M., Tomlinson, P. K., and Maunder, M. N. 2010a. Exploratory analysis of spatial-temporal patterns in length-frequency data: an example of distributional regression trees. Fisheries Research, 102: 323–326.

Liaw, A., and Wiener, M. 2002. Classification and Regression by randomForest. R News, 2(3): 18–22.

Libungan, L. A., Óskarsson, G. J., Slotte, A., Jacobsen, J. A., and Pálsson, S. 2015. Otolith shape: A population marker for Atlantic herring *Clupea harengus*. Journal of Fish Biology, 86: 1377–1395.

Libungan, L. A., and Pálsson, S. 2015. ShapeR: An R package to study otolith shape variation among fish populations. PLoS ONE, 10(3): e0121102.

Lorrain, A., Pethybridge, H., Cassar, N., Receveur, A., Allain, V., Bodin, N., Bopp, L., et al. 2020. Trends in tuna carbon isotopes suggest global changes in pelagic phytoplankton communities. Global Change Biology, 26: 458–470.

Macdonald, J. I., Farley, J. H., Clear, N. P., Williams, A. J., Carter, T. I., Davies, C. R., and Nicol, S. J. 2013. Insights into mixing and movement of South Pacific albacore *Thunnus alalunga* derived from trace elements in otoliths. Fisheries Research, 148: 56–63.

Montes, I., Iriondo, M., Manzano, C., Arrizabalaga, H., Jiménez, E., Pardo, M. Á., Goñi, N., et al. 2012. Worldwide genetic structure of albacore *Thunnus alalunga* revealed by microsatellite DNA markers. Marine Ecology Progress Series, 471: 183–191.

Moore, B. R., Lestari, P., Cutmore, S. C., Proctor, C., Lester, R. J. G., and Watson, J. 2019. Movement of juvenile tuna deduced from parasite data. ICES Journal of Marine Science, 76: 1678–1689.

Moore, B. R., Bell, J. D., Evans, K., Farley, J., Grewe, P. M., Hampton, J., Marie, A. D., et al. 2020a. Defining the stock structures of key commercial tunas in the Pacific Ocean I: Current knowledge and main uncertainties. Fisheries Research, 230: 105525.

Moore, B. R., Adams, T., Allain, V., Bell, J. D., Bigler, M., Bromhead, D., Clark, S., et al. 2020b. Defining the stock structures of key commercial tunas in the Pacific Ocean II: Sampling considerations and future directions. Fisheries Research, 230: 105524.

Nason, G. 2022. wavethresh: Wavelets Statistics and Transforms. R package version 4.7.2, https://CRAN.R-project.org/package=wavethresh.

Oksanen, J., Simpson, G., Blanchet, F., Kindt, R., Legendre, P., Minchin, P., O'Hara, R., et al. 2022. vegan: Community Ecology Package. R package version 2.6-4, https://CRAN.R-project.org/package=vegan.

Pecoraro, C., Babbucci, M., Franch, R., Rico, C., Papetti, C., Chassot, E., Bodin, N., et al. 2018. The population genomics of yellowfin tuna (*Thunnus albacares*) at global geographic scale challenges current stock delineation. Scientific Reports, 8: 13890.

Porch, C., Kleiber, P., Turner, S., Sibert, J., Bailey, R., and Cort, J. 1998. The efficacy of VPA models in the presence of complicated movement patterns. Col. Vol. Sci. Pap. ICCAT, 50: 591–622.

Pilling, G., and Brouwer, S., 2018. Report from the SPC pre-assessment workshop, Noumea, April 2018. SC14/SA-IP-01. Fourteenth Regular Session of the Scientific Committee of the Western and Central Pacific Fisheries Commission. Busan, South Korea, 8-16 August 2018. https://meetings.wcpfc.int/node/10583

Potts, J., Castillo-Jordán, C., Day, J., Hamer, P., and Teears, T. 2024. Analysis of Longline Size Frequency Data for the 2024 Southwest Pacific Striped Marlin and South Pacific Albacore Assessments. SC20/SA-IP-03. Twentieth Regular Session of the Scientific Committee of the Western and Central Pacific Fisheries Commission. Manila, Philippines, 14-21 August 2024. https://meetings.wcpfc.int/node/23064

Punt, A. E. 2019. Spatial stock assessment methods: A viewpoint on current issues and assumptions. Fisheries Research, 213: 132–143.

R Core Team 2023. R: A Language and Environment for Statistical Computing. R Foundation for Statistical Computing, Vienna, Austria. https://www.R-project.org/.

Sakamoto, T., Komatsu, K., Shirai, K., Higuchi, T., Ishimura, T., Setou, T., Kamimura, Y., et al. 2019. Combining microvolume isotope analysis and numerical simulation to reproduce fish migration history. Methods in Ecology and Evolution, 10: 59–69.

Scutt Phillips, J., Sen Gupta, A., Senina, I., van Sebille, E., Lange, M., Lehodey, P., Hampton, J., et al. 2018. An individual-based model of skipjack tuna (*Katsuwonus pelamis*) movement in the tropical Pacific ocean. Progress in Oceanography, 164: 63–74.

Senina, I. N., Lehodey, P., Hampton, J., and Sibert, J. 2020. Quantitative modelling of the spatial dynamics of South Pacific and Atlantic albacore tuna populations. Deep-Sea Research Part II: Topical Studies in Oceanography, 175: 104667.

SHOU, ANCORS, and SPC. 2024. South Pacific Albacore: Science, Data and Climate Change Workshop Report. SPA-RM-IWG05-2024/04. Wollongong, Australia, 29-30 April 2024. https://meetings.wcpfc.int/node/22751

SPC-OFP and CSIRO 2024. Progress Towards a Close-Kin Mark-Recapture Application to South Pacific Albacore (Project 100c). SC20/SA-WP-09. Twentieth Regular Session of the Scientific Committee of the Western and Central Pacific Fisheries Commission. Manila, Philippines, 14-21 August 2024. https://meetings.wcpfc.int/node/23123

Taillebois, L., Davenport, D., Barton, D. P., Crook, D. A., Saunders, T., Hearnden, M., Saunders, R. J., et al. 2021. Integrated analyses of SNP-genotype and environmental data in a continuously distributed snapper species (*Lutjanus johnii*, Bloch, 1792) reveals a mosaic of populations and a challenge for sustainable management. ICES Journal of Marine Science, 78: 3212–3229.

Takagi, M., Okamuraet, T., Chow, S., and Taniguchi, N. 2001. Preliminary study of albacore (*Thunnus alalunga*) stock differentiation inferred from microsatellite DNA analysis. Fishery Bulletin, 99: 697–701.

Teears, T., Castillo-Jordán, C., Davies, N., Day, J., Hampton, J., Magnusson, A., Xu, H., Vidal, T., Williams, P., and Hamer, P. 2024. Stock Assessment of South Pacific albacore. SC20/SA-WP-02. Twentieth Regular Session of the Scientific Committee of the Western and Central Pacific Fisheries Commission. Manila, Philippines, 14-21 August 2024. https://meetings.wcpfc.int/node/23119

Tremblay-Boyer, L., Hampton, J., McKechnie, S., and Pilling, G. 2018a. Stock assessment of South Pacific albacore tuna. SC14/SA-WP-05. Fourteenth Regular Session of the Scientific Committee of the Western and Central Pacific Fisheries Commission. Busan, South Korea, 8-16 August 2018. https://meetings.wcpfc.int/node/10740

Tremblay-Boyer, L., McKechnie, S., and Pilling, G. 2018b Background analysis for the 2018 stock assessment of South Pacific albacore tuna. SC14/SA-IP-07. Fourteenth Regular Session of the Scientific Committee of the Western and Central Pacific Fisheries Commission. Busan, South Korea, 8-16 August 2018. https://meetings.wcpfc.int/node/10748

Vaux, F., Bohn, S., Hyde, J. R., and O'Malley, K. G. 2021. Adaptive markers distinguish North and South Pacific albacore amid low population differentiation. Evolutionary Applications, 14: 1343–1364.

Vignon, M. 2015. Disentangling and quantifying sources of otolith shape variation across multiple scales using a new hierarchical partitioning approach. Marine Ecology Progress Series, 534: 163–177.

Vignon, M., and Morat, F. 2010. Environmental and genetic determinant of otolith shape revealed by a non-indigenous tropical fish. Marine Ecology Progress Series, 411: 231–241.

Williams, A. J., Allain, V., Nicol, S. J., Evans, K. J., Hoyle, S. D., Dupoux, C., Vourey, E., et al. 2015. Vertical behavior and diet of albacore tuna (*Thunnus alalunga*) vary with latitude in the South Pacific Ocean. Deep-Sea Research Part II: Topical Studies in Oceanography, 113: 154–169.

Williams, A. J., Farley, J. H., Hoyle, S. D., Davies, C. R., and Nicol, S. J. 2012. Spatial and sex-specific variation in growth of albacore tuna (*Thunnus alalunga*) across the South Pacific Ocean. PLoS ONE, 7(6): e39318.

Xu, H., and Lennert-Cody, C. E. 2023. FishFreqTree: IATTC's regression tree R package for fisheries' size frequency data. R package v. 3.3.2.

Appendix

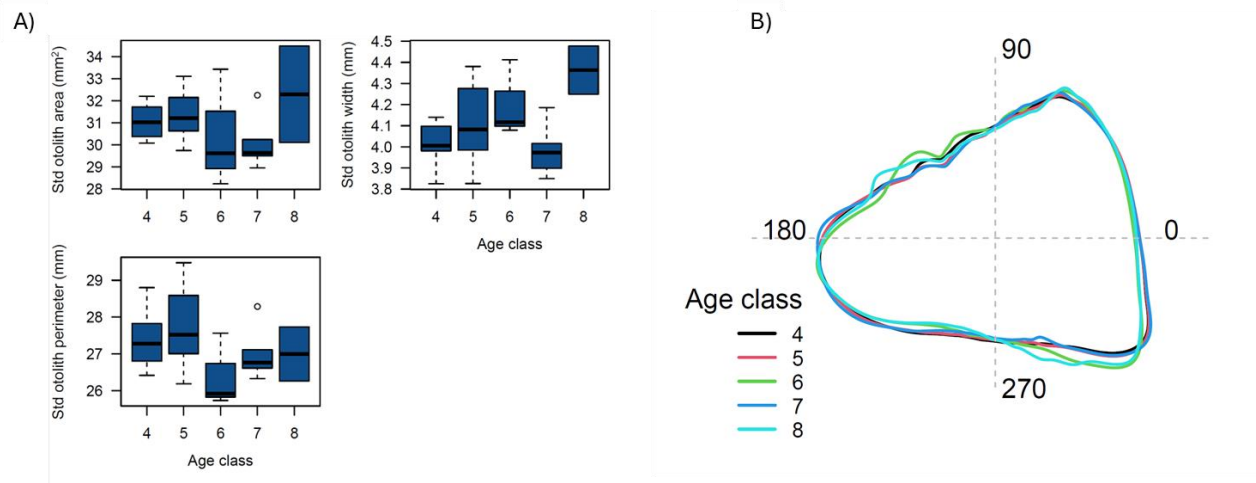

Figure A1. Visualisation of otolith shape variation among age classes in FP. (A) Box plots summarising the distribution of standardised shape measurements per age class. Thick black horizontal lines are the median values for each box and the lower (Q1) and upper (Q3) quartiles (box limits) are shown. Upper whiskers represent the smaller of the maximum value of the variable and Q3 + 1.5 × interquartile range, and lower whiskers the larger of the minimum value of the variable and Q1 - 1.5 × interquartile range. (B) Mean reconstructed otolith outline for each age class. Numbers refer to angles in degrees.

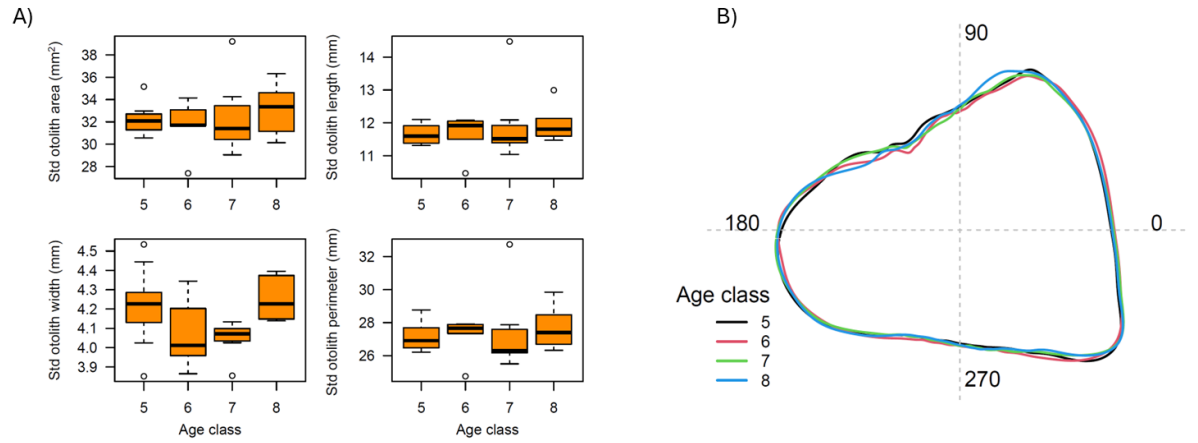

Figure A2. Visualisation of otolith shape variation among age classes in NC. All details for A) and B) as in Figure A1.

DNA extraction and sequencing, conducted by Diversity Arrays Technology

Tissue samples were provided to Diversity Arrays Technology as part of a larger sequencing effort.

Genomic DNA was extracted and processed for reduced representation library construction, sequenced and genotyped using DArT PL's patented protocol, DArTseq™. Some procedures were proprietary, but reasonably detailed descriptions are available (Sansaloni et al. 2011; Kilian et al. 2012; Cruz et al. 2013; Ren et al. 2015). Briefly, DNA was extracted in the DArT PL laboratory, presumably with a basic CTAB protocol. Purified DNA then underwent genome complexity reduction with a double restriction digest using methylation-sensitive restriction enzymes, which is a method DArT PL has previously optimised for tuna samples. Adaptors that include variable barcode sequences and Illumina flowcell attachment sequences were ligated to fragments. PCR amplified only mixed fragments in a sequence of initial denaturation at 94°C for one minute, followed by 30 cycles of 94°C for 20 seconds, 58°C for 30 seconds, and 72°C for 45 seconds. A final extension step took 7 minutes at 72°C. Libraries were bulked and applied to c-Bot bridge PCR, then single-end sequenced on an Illumina Novaseq6000 platform for 83 cycles.

Raw reads obtained following sequencing were processed using DArTech PL's proprietary analytical pipelines according to Kilian et al. (2012). The pipelines filter away poor-quality sequences, demultiplex reads, groom out singletons and other low quality tags, and eventually apply DArTsoft14 variant calling algorithms. SNP markers were further filtered for paralogs, low read depth and suspect call quality. Based on this dataset, we flagged a variety of samples that were either not relevant to the current analysis or did not sequence normally. The remaining raw sequencing reads were then resubmitted to the DArTsoft14 pipeline in order to call genotypes that are study-specific.

Additional quality filtering and development of final datasets

The final dataset provided by DArTech PL included 121105 loci and 131 samples in three sample groups: NC_June (37 samples taken in New Caledonian waters in June 2022), NC_Nov (47 samples from New Caledonia in November 2022) and FP_Nov (47 samples from French Polynesia in November 2022). We proceeded to filter the original dataset twice. Filtering was either done manually or using the DartRverse package in R. Specifics about number of loci filtered at each step in either dataset are available in Table 1, below.

The first, primary dataset removed loci based on the following quality filters thresholds calculated globally across all three sample groups:

- all loci per contig except that with the highest information content
- loci with a call rate < 95%
- with a read depth below 12x or above 100x
- more than 50% heterozygosity
- minor allele count lower than 5x
- deviation from Hardy-Weinberg equilibrium in more than one sample group after adjustment of associated p-values using the (Benjamini and Yekutieli 2001) correction method
- loci in linkage disequilibrium with a correlation $r^2 > 0.2$, also informed by metadata provided by DArTech after an attempt to map loci to an available bluefin tuna reference genome (part of the genotyping pipeline)

A second dataset was created to capture loci that are F_{ST} outliers. To do this, we adjusted our filtering thresholds slightly to include more loci with rare alleles, which are more likely to be flagged in F_{ST} outlier analyses but carry higher risk of being a sequencing error. We simultaneously increased other quality filter thresholds to ensure we did not retain erroneous loci. Furthermore, we only considered samples from FP_Nov and NC_Nov to ensure selected loci were explicitly informative for this spatial

comparison. Once all filtering and selection processes were complete, we re-incorporated the NC_June data for the same loci. Specifically, we filtered based on:

- all loci per contig except that with the highest information content
- loci with a call rate < 95%
- with a read depth below 15x or above 100x
- more than 50% heterozygosity
- minor allele count lower than 3x
- deviation from Hardy-Weinberg equilibrium in more than one sample group after adjustment of associated p-values using the Benjamini & Yekutieli (2001) correction method
- loci in linkage disequilibrium with a correlation $r^2 > 0.2$, also informed by metadata provided by DArTech after an attempt to map loci to an available bluefin tuna reference genome (part of the genotyping pipeline)

The resulting dataset was then submitted to four different programs that detect F_{ST} outlier loci.

- Bayescan (Foll and Gaggiotti, 2008): combines a Dirichlet distribution model with a Bayesian method to estimate each's loci's posterior probability. It is one of the most frequently cited F_{ST} outlier detection programs in the literature (2886 citations at the time of writing).
- HacDivSel, Exterme Outlier Set test (Carvajal-Rodríguez, 2017): uses a two-step G_{ST} outlier test that minimises false positive discovery rate in scenarios of moderate or high migration rates, which makes it particularly relevant to tuna.
- Outflank (Whitlock and Lotterhos, 2015): uses a revised Lewontin-Krakauer model and was specifically designed to be more flexible when defining the neutral distribution of loci for a study. This is again helpful given the uncertain population model of tuna and demonstrated high neutral diversity.
- PCAdapt (Luu et al. 2016): tests for structure by principal component analysis prior to testing for FST outlier loci. It is particularly geared toward identifying local adaptation as opposed to other drivers of adaptation and is consciously designed to handle admixed individuals, which are additional likely scenarios for tuna.

All software programs were run using default settings, apart from specifying a false discovery rate of 5% where applicable. Outflank and PCAdapt also allow modification of the minimum minor allele frequency per loci, which we specified as close to zero as each software allows, in an effort to preserve adaptive structure driven by rare alleles (Linck and Battey, 2019).

Loci were included in the secondary dataset if they were flagged by any of the considered software programs. We also ran analyses using a dataset that only retained loci identified by two or more software programs, but this produced the same trends and suffered from reduced statistical power.

Table A1. loci retained at each filtering step for the two datasets, including FST outlier selection specific to the secondary dataset.

Filter type	Dataset	
	Primary	Secondary
Quality Filters		
Original	121105	121105
Replicates per contig	61705	61705
Call rate	19940	19566
Read depth	15704	14948
Heterozygosity	15627	14865
Minor allele count	6891	6797
Hardy Weinberg equilibrium	6890	6793
Linkage disequilibrium	6756	6730
FST outliers		
Bayescan	NA	23
HacDivSel	NA	74
Outflank	NA	38
PCAdapt	NA	21

While F_{ST} outlier status is often used as a proxy to identify loci that are under adaptive pressure, our study design using only two sample groups makes it difficult to determine what external forces might be associated with any flagged loci. We therefore treat this dataset more as a cherry-picked panel of loci to help distil otherwise very subtle patterns reported using the primary dataset.

Further details about genetic analysis methods

We provide coding details here for reproducing all genetic analyses conducted in programs. They are ordered as they appear in the main text. All processes run in R use v 4.2.2 (R Core Team, 2022).

- Ho, unbiased He (reported as µHe), F_{IS} —calculated using *DartR.base* package v 0.65 in R (Gruber et al. 2018; Mijangos et al. 2022), command 'gl.report.heterozygosity'
- Pairwise F_{ST}—*StAMPP* package v 1.6.3 in R (Pembleton et al. 2013), 'stamppFst' specifying 'nboots=10000'
- Pairwise F_{ST} p values—adjusted for multiple comparisions using *stats* package v 4.5.0 in R (R Core Team, 2022), command 'p.adjust' specifying 'method = 'BY'' for the Benjamini & Yekutieli (2001) correction method
- DAPC—*adegenet* package v 2.1.10 in R (Jombart, 2008; Jombart and Ahmed, 2011), using command 'dapc' and specifying number of principal components and discriminant functions interactively. Number of PC's was informed by cross validation
- DAPC cross validation—*adegenet*, using command 'xvalDapc' on a genind object transformed into a matrix (via R base command 'tab', specifying 'Na.method='mean') and reporting output [6], Number of PCs Achieving Lowest MSE, as the number of PC's to use.
- STRUCTURE—self-contained software package v 2.3 (Pritchard et al. 2000) run in the R environment via package *strataG* v 2.5.01 (Archer et al. 2017), command 'structureRun' specifying 'k.range=1:5, num.k.rep=5, burnin=5000, numreps=50000'
- STRUCTURE k-selection—*StrataG*, command 'evanno' specifying the output of 'structureRun'; appropriate k value selected based on indicators recommended in (Pritchard, Stephens, and Donnelly 2000; Evanno, Regnaut, and Goudet 2005) namely picking the first

value of k to produce a plateau in value meanLnP(K) (the mean log probability of results at a given k value) of and/or a spike in Δk (change in the log probability value between successive k's). Failure of results to conform to expected outputs patterns for either metric was interpreted as support for k=1.

- STRUCTURE visualisation—*DartR.popgen* v 0.3.2 R (Gruber et al. 2018; Mijangos et al. 2022) (wrapping functions from *StrataG*), command 'gl.plot.structure' specifying the output of 'structureRun' and 'K=2' for the LUPS dataset.
- ADMIXTURE—self-contained software v 1.3.0 (Alexander et al. 2009; Zhou et al. 2011), run via command line './admixture' specifying '--cv FILE.bed k|tee logk.out' over sequential k-values = 1-10. Cross-validation values are saved into logk.out files and retrieved to compare and select appropriate k based on lowest CV.
- ADMIXTURE visualisation—First augment the ADMIXTURE output q-file for the selected k value ('outfile.Q.[k]') to include a new column 1, labelled 'orig.pop' and populated with the group name per individual. Then submit to *strataG* in R, command 'structurePlot', specifying 'pop.col=1, prob.col=2, sort.probs=FALSE, horiz=FALSE, type='bar', legend.position="none", col=rainbow(k)).
- DAPC-k means clustering—*adegenet*, using command 'find.clusters' and interactively selecting to keep all available principal components and discriminant functions. Function returns output$Kstat with Bayesian Information Criterion values for k=1-20 and the lowest BIC value used to identify the most appropriate k.
- StockR individual assignment—*StockR* package v 1.0.76 in R (Foster et al. 2018), 'stockSTRUCTURE' run iteratively specifying K=1-5 to fit the data to between 1 and 5 underlying populations, 'stockBOOT' specifying B=500 to test the confidence of individual assignments over 500 bootstraps, and 'plot.stockBOOT.object' specifying CI.width=0.95 to manipulate the scaling of color intensities in returned visuals.

Appreciable differences between clustering programs

As with F_{ST} outlier selection programs, there are an increasing number of software programs that provide genetic clustering recommendations with different sensitivities and underlying assumptions. We provide a few more insights into each of our selected algorithms here. Exact commands are provided in the section above.

- STRUCTURE (Pritchard et al. 2000): is the most cited clustering program in the literature (over 38000 citations of (Pritchard, Stephens, and Donnelly 2000) at the time of writing). It uses a Bayesian approach and Markov Chain Monte Carlo estimation to calculate each individual's probability of assignment to each cluster within a given k. Thanks to the base program's popularity, a number of additional programs have been developed to improve interpretation and readability of the output, and compensate for a number of acknowledged blind spots (which leads to our incorporation of recommendations by (Evanno, Regnaut, and Goudet 2005)). A drawback of the program is its underlying population model assumptions, some of which are not well fitted to a tuna's life history. Regardless, we choose to use the software for the sake of comparison with existing literature.
- ADMIXTURE (Alexander et al. 2009; Zhou et al. 2011): uses the same basic model as STRUCTURE, but with a block relaxation algorithm and maximum likelihood framework to assign individuals to the given number of clusters (k). It is specifically advertised as a follow-up to STRUCTURE that is much faster to run and handles admixed individuals better.
- Adegenet (Jombart, 2008; Jombart and Ahmed, 2011): As part of conducting a DAPC, adegenet also provides a computation-efficient clustering approach that applies *k*-means clustering to a PCA-transformed dataset. In contrast to STRUCTURE, it does not require selection of a population structure model, therefore allowing for much more fluid applications. Although the adegenet package does also provide options to visualise confidence of individual assignment to their group, the software manual (Jombart and

Collins, 2015) warns against using this feature on data re-grouped according to clustering recommendations, as this would only create circular validation. We therefore only present the BIC results of *k*-means clustering and a complete DAPC scatterplot of samples in their *a priori* groups.

- StockR (Foster et al. 2018): first employs *k*-means clustering similar to adegenet, followed by a final classification by EM-algorithm (expectation-maximum) approach and confidence in each individual's assignment measured using Bayesian bootstraps. This is one of the few programs designed explicitly to clarify stock delineations, as opposed to identifying founder populations. As such, it is less prescriptive about the underlying *k*-value, but can reveal potentially relevant substructure at diverse *k*'s. It is therefore only reported for the LUPS dataset, where there is sufficient external evidence to support *k*=2.

References

Alexander, D., Novembre, J., and Lange, K. 2009. Fast model-based estimation of ancestry in unrelated individuals. Genome research, 19: 1655–64.

Archer, F. I., Adams, P. E., and Schneiders, B. B. 2017. stratag: An r package for manipulating, summarizing and analysing population genetic data. Molecular Ecology Resources, 17: 5–11.

Benjamini, Y., and Yekutieli, D. 2001. The control of the false discovery rate in multiple testing under dependency. The Annals of Statistics, 29: 1165–1188.

Carvajal-Rodríguez, A. 2017. HacDivSel: Two new methods (haplotype-based and outlier-based) for the detection of divergent selection in pairs of populations. PLOS ONE, 12: e0175944.

Cruz, V. M. V., Kilian, A., and Dierig, D. A. 2013. Development of DArT Marker Platforms and Genetic Diversity Assessment of the U.S. Collection of the New Oilseed Crop Lesquerella and Related Species. PLoS ONE, 8: e64062.

Evanno, G., Regnaut, S., and Goudet, J. 2005. Detecting the number of clusters of individuals using the software STRUCTURE: A simulation study. Molecular Ecology, 14: 2611–2620.

Foll, M., and Gaggiotti, O. 2008. A Genome-Scan Method to Identify Selected Loci Appropriate for Both Dominant and Codominant Markers: A Bayesian Perspective. Genetics, 180: 977–993.

Foster, S. D., Feutry, P., Grewe, P. M., Berry, O., Hui, F. K. C., and Davies, C. R. 2018. Reliably discriminating stock structure with genetic markers: Mixture models with robust and fast computation. Molecular Ecology Resources, 18: 1310–1325.

Gruber, B., Unmack, P. J., Berry, O., and Georges, A. 2018. dartR: an R package to facilitate analysis of SNP data generated from reduced representation genome sequencing. Molecular Ecology Resources, 18: 691–699.

Jombart, T. 2008. Adegenet: A R package for the multivariate analysis of genetic markers. Bioinformatics, 24: 1403–1405.

Jombart, T., and Ahmed, I. 2011. adegenet 1.3-1: new tools for the analysis of genome-wide SNP data. Bioinformatics, 27: 3070–3071.

Jombart, T., and Collins, C. 2015. A tutorial for Discriminant Analysis of Principal Components (DAPC) using adegenet 1.3-4.

Kilian, A., Wenzl, P., Huttner, E., Carling, J., Xia, L., Blois, H., Caig, V., *et al.* 2012. Diversity Arrays Technology: A Generic Genome Profiling Technology on Open Platforms. *In* Data Production and Analysis in Population Genomics: Methods and Protocols, pp. 67–89. Humana Press, Totowa, NJ.

Linck, E., and Battey, C. J. 2019. Minor allele frequency thresholds strongly affect population structure inference with genomic data sets. Molecular Ecology Resources, 19: 639–647.

Luu, K., Bazin, E., and Blum, M. G. B. 2016. pcadapt : an R package to perform genome scans for selection based on principal component analysis. Molecular Ecology Resources, 17: 67–77.

Mijangos, J. L., Gruber, B., Berry, O., Pacioni, C., and Georges, A. 2022. dartR v2: An accessible genetic analysis platform for conservation, ecology and agriculture. Methods in Ecology and Evolution, 13: 2150–2158.

Pembleton, L. W., Cogan, N. O. I., and Forster, J. W. 2013. StAMPP: An R package for calculation of genetic differentiation and structure of mixed-ploidy level populations. Molecular Ecology Resources, 13: 946–952.

Pritchard, J., Stephens, M., and Donnelly, P. 2000. Inference of Population Structure Using Multilocus Genotype Data. Genetics, 155: 945–959.

R Core Team. 2022. R: A language and environment for statistical computing. Vienna, Austria.

Ren, R., Ray, R., Li, P., Xu, J., Zhang, M., Liu, G., Yao, X., *et al.* 2015. Construction of a high-density DArTseq SNP-based genetic map and identification of genomic regions with segregation distortion in a genetic population derived from a cross between feral and cultivated-type watermelon. Molecular Genetics and Genomics, 290: 1457–1470.

Sansaloni, C., Petroli, C., Jaccoud, D., Carling, J., Detering, F., Grattapaglia, D., and Kilian, A. 2011. Diversity Arrays Technology (DArT) and next-generation sequencing combined: genome-wide, high throughput, highly informative genotyping for molecular breeding of Eucalyptus. BMC Proceedings, 5: P54.

Whitlock, M. C., and Lotterhos, K. E. 2015. Reliable Detection of Loci Responsible for Local Adaptation: Inference of a Null Model through Trimming the Distribution of F(ST). The American Naturalist, 186: S24–S36.

Zhou, H., Alexander, D., and Lange, K. 2011. A quasi-Newton acceleration for high-dimensional optimization algorithms. Statistics and Computing, 21: 261–273.